JAAS

ROYAL SOCIETY OF CHEMISTRY

PAPER

View Article Online
View Journal | View Issue

Cite this: *J. Anal. At. Spectrom.*, 2021, **36**, 1768

The application of tetramethylammonium hydroxide for generating atmospheric pressure glow discharge in contact with alkalized flowing liquid cathode solutions – evaluation of the analytical performance†

Monika Gorska * and Pawel Pohl

The analytical performance of atmospheric pressure glow discharge (APGD) generated in contact with the alkalized flowing liquid cathode (FLC) solutions for the determination of Zn, Cd, Ag, Pb, Ga, Ca, In, Tl, and Rb by optical emission spectrometry (OES) was studied. Tetramethylammonium hydroxide (TMAH) was applied for sample alkalization. The emission spectra of APGD generated in contact with the alkalized and acidified FLC solutions were compared and discussed. The optimization of the most crucial operating conditions, *i.e.*, the discharge current, the solution flow rate, and the TMAH concentration, was performed. Furthermore, the analytical figures of merit were determined under the optimized conditions. Finally, the impact of the presence of selected low molecular weight organic compounds (LMWOCs) as well as commonly occurring foreign cations (*i.e.*, Al^{3+}, Ca^{2+}, Cr^{3+}, Cu^{2+}, Fe^{3+}, K^{+}, Mg^{2+}, Mn^{2+}, Na^{+}, Sn^{2+}, and Zn^{2+}) on the analyte signals was assessed. Although some variations between the results obtained for the alkalized and acidified solutions were found, the obtained outcomes led us to a general conclusion about the pH-independence of the excitation conditions in the discharge. Nevertheless, possible analyte reactions taking place in alkalized solutions and/or with TMAH should be taken into consideration. The detection limits (DLs) of Zn, Cd, Ag, Pb, Ga, Ca, In, Tl and Rb were similar or better, compared to the ones reported for other FLC-APGD systems, and equal to 9.7, 10, 0.81, 28, 3.0, 33, 1.0, 0.83, and 0.35 μg L^{-1}, respectively. Though the developed FLC-APGD system could not be applied for the determination of certain elements (namely K, Mg, and Na), the determined DLs for the studied elements, along with relatively wide ranges of the calibration curves linearity (up to 10 mg L^{-1}) and good precision (RSD close to 2%, on average), make the proposed FLC-APGD method a suitable alternative to both other microplasma techniques as well as conventionally applied large-scale instrumentation.

Received 29th April 2021
Accepted 29th June 2021

DOI: 10.1039/d1ja00148e

rsc.li/jaas

1. Introduction

The reliable determination of metals in diverse kinds of samples, including solid ones, is of great importance in analytical chemistry due to either their potentially adverse impact on human health or their nutritional quality. Several commercially available spectrometric techniques are applied for this purpose and they include atomic absorption spectrometry (AAS), atomic fluorescence spectrometry (AFS), inductively coupled plasma optical emission spectrometry (ICP-OES), microwave induced plasma optical emission spectrometry (MIP-OES) or inductively coupled plasma mass spectrometry (ICP-MS). These techniques assure detection limits (DLs) ranging from relatively low (AAS) to ultra-low (ICP-MS), at least 3 orders of magnitude of the linearity ranges of calibration curves, and good sensitivity and precision. Moreover, some of the abovementioned techniques (namely ICP-OES, MIP-OES, and ICP-MS) also allow us to perform multi-element analyses. Nonetheless, the application of the techniques listed above involves certain disadvantages such as bulky and complex instrumentation as well as high gas and power consumption, which, in effect, translates into their high utilization costs. On this account, the attention of many researchers has been directed to the development of miniaturized plasma sources which are hoped to provide the analytical characteristics similar to those of the currently used bulky instruments but with simplified instrumentation and at low costs.[1–5]

Numerous examples of such devices have been reported so far, for the element analysis by OES, *e.g.*, electrolyte cathode

Faculty of Chemistry, Division of Analytical Chemistry and Chemical Metallurgy, Wroclaw University of Science and Technology, Wybrzeze Stanislawa Wyspianskiego 27, 50-370 Wroclaw, Poland. E-mail: monika.gorska@pwr.edu.pl

† Electronic supplementary information (ESI) available. See DOI: 10.1039/d1ja00148e

discharge (ELCAD),[6] discharge on boiling in a channel (DBC),[7] solution cathode glow discharge (SCGD),[8] flowing liquid cathode – atmospheric pressure glow discharge (FLC-APGD),[9] solution anode glow discharge (SAGD),[10] flowing liquid anode – atmospheric pressure glow discharge (FLA-APGD),[11] liquid drop anode – atmospheric pressure glow discharge (LDA-APGD),[12] or hanging drop electrode – atmospheric pressure glow discharge (HDE-APGD).[3]

Among the abovementioned excitation sources, FLC-APGD, along with similar systems such as ELCAD and SCGD, is one of the most commonly developed ones.[13] It is a very promising excitation source as its application provides numerous advantages including a simple atomic spectrum and relatively low background fluctuations along with acceptable sensitivity of analytical lines of elements, resulting in DLs of these elements comparable to those achievable with flame atomic absorption spectrometry (FAAS), ICP-OES or MIP-OES. Moreover, it offers all the advantages ascribed to miniaturized plasma sources, *i.e.*, small size, no requirement for the use of noble gases, and stable operation at low electric current power consumption, which translates into significantly reduced operating costs.[14,15]

As the FLC solution is a part of the electrical circuit, it needs to provide appropriate electrical conductivity. For this purpose, the FLC solutions are commonly acidified with different acids, *i.e.*, HNO_3,[16–21] HCl,[16,21,22] H_2SO_4,[17,22,23] HF,[24] and H_3PO_4.[25] Among the abovementioned acids, the use of HNO_3 is preferred for sample acidification as it does not form any precipitate, and it is extensively used for the wet digestion procedure, during sample preparation.[13] In the vast majority of cases, the optimal solution pH is established to be equal to 1, which assures both stable discharge operation as well as the highest intensity of the analyte atomic lines.[3,20–22,26]

The application of solutions of reagents other than acids, *e.g.*, bases or salts, was rarely reported for any type of microdischarge. Mezei *et al.*[27] investigated the impact of different supporting electrolytes (namely HNO_3, HCl, H_2SO_4, KNO_3, KCl, and K_2SO_4) on the Cd signal intensity for the ELCAD system. They noted that the Cd signal increased over the whole range of the studied acid concentrations (up to 0.2 eq L^{-1}), while in the case of their salts, it was noted to increase only up to 0.03 eq L^{-1} and then remained the same or dropped. Zuev *et al.*[28] investigated the impact of increasing concentrations of LiCl, NaCl, NH_4Cl, NaOH, H_2SO_4, HCl, HBr, and HNO_3 on the signal intensity of Ca, Cs, Ga, In, Na, Rb, and Sr for the DBC system. Generally, they observed a signal increase for all analytes at first and its subsequent drop with the further increase of the electrolyte concentration. They noted that this tendency was similar for all supporting electrolytes, regardless of their kind. Similar tendencies were observed by Yagov *et al.*,[29] who investigated the impact of increasing concentrations of HNO_3, H_2SO_3, NH_4NO_3, $Zn(NO_3)_2$, KCl, and tetramethylammonium hydroxide (TMAH) on the signal intensity of Ga, In, Li, Na, and Pb in drop-spark discharge (DSD). Only in the case of TMAH, the signal intensity of the analytes increased over the whole studied concentration range; however, this range was much shorter than that for the other electrolytes. The authors concluded that acids do not possess any specific properties as supporting electrolytes and, in some cases, the analytical response for alkaline media may be even stronger than that for acidic solutions.

TMAH is a strongly alkaline and water soluble reagent, solubilizing different kinds of tissues.[30] It is commonly used in many different processes, *e.g.*, etching,[31] extraction,[32] pyrolysis-gas chromatography,[33] and thermochemolysis.[34] Apart from that, it is also applied for the decomposition of samples of different matrices, before their analysis with the aid of conventional large-scale instrumentation.[30,35–38] As compared to the use of acids, the solubilization of sample components with TMAH is simpler and faster than that with acids, usually efficient at room temperature, minimizing the risk of volatile analyte losses, and requires only small portions of the reagent.[30,35]

To the best of our knowledge, there is no comprehensive study focusing on the generation of FLC-APGD (and other similar systems such as ELCAD or SCGD) in contact with alkalized solutions. Therefore, the aim of this work was to replace HNO_3, extensively used for the acidification of FLC solutions, with TMAH and study the FLC-APGD system in reference to its spectroscopic behavior and analytical performance.

To reach this goal, at first, the emission spectra of the FLC-APGD system generated in contact with acidified and alkalized FLC solutions were recorded and compared. Further, the optimization of the crucial working parameters was performed for selected elements transported to the discharge from a solution alkalized with TMAH. Under the optimized conditions, the analytical figures of merit, in terms of the DLs, the linearity ranges of the calibration curves, and the measurement precision, were evaluated. Subsequently, the effect of the addition of low molecular weight organic compounds (LMWOCs) on the analyte signal intensity was investigated. Finally, the impact of selected foreign ions on the analyte signal intensities was studied in order to evaluate the suitability of the proposed methodology for real sample analysis by OES. The results were discussed comprehensively and partially compared with those obtained for the system conventionally operated in contact with acidified FLC solutions.

2. Experimental

2.1. Instrumentation

A schematic drawing of the developed FLC-APGD system is presented in Fig. 1. The discharge was sustained in an open-to-air chamber between a tungsten rod (OD 2 mm, length 170 mm) and a cathode solution flowing through a tungsten tube (OD/ID 3/2 mm, length 100 mm). The tungsten tube and the tungsten rod were oriented vertically to each other. The sample solutions alkalized with TMAH, which served as the FLC, were pumped through the tungsten tube by means of a 3-channel REGLO ICC peristaltic pump (Ismatec, USA) at different flow rates being set in the 1.0–4.0 mL min^{-1} range. As the solution reached the tungsten tube's top, it flowed down to a Teflon reservoir, from which it was pumped out. The tungsten rod served as a pin-type anode. The distance between the solution surface and the anode rod (so-called discharge gap) was set to approximately 1.5

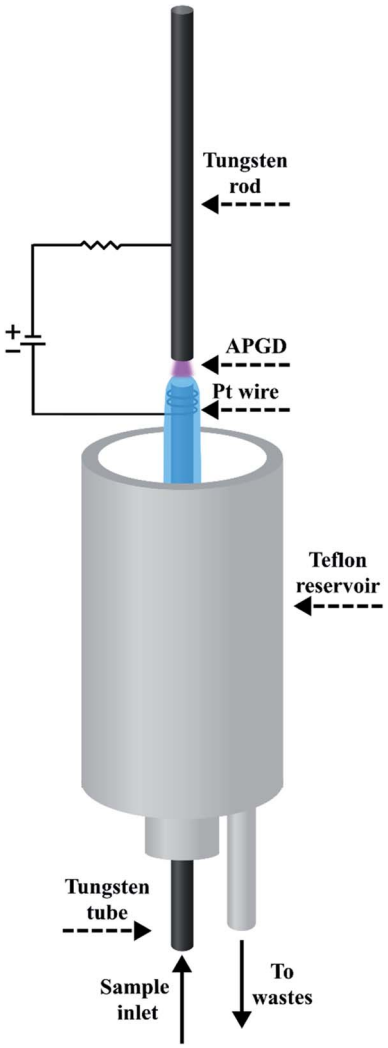

Fig. 1 A schematic drawing of the developed FLC-APGD system.

mm. The electrical contact was provided directly to the tungsten rod and with the aid of a platinum spiral wrapped around the tungsten tube. A voltage of around 1000 V was applied to both electrodes from a HV dc power supply (model DP50H-024PH, DSC-Electronics, Germany). Its exact value depended on the applied sample flow rate, the discharge current, and the TMAH concentration. To stabilize the discharge, a 6.9 kΩ ballast resistor was connected to the circuit.

The radiation emitted by APGD was imaged (1 : 1) on the entrance slit (10 μm) of a Shamrock 500i imaging spectrometer (Andor, UK), using an achromatic quartz lens (f = 80). The spectrometer was equipped with a holographic grating (1800 lines mm^{-1}) and a Newton DU-920P-OE UV-Vis CCD camera (Andor, UK). The integration time was 10 s during all experiments and intensities of atomic emission lines of the studied elements were background corrected. The following wavelengths of the analytical lines were traced during the experiments: Zn (213.9 nm), Cd (228.8 nm), Fe (248.3 nm), Hg (253.7 nm), Mg (285.2 nm), Ag (338.3 nm), Pb (368.3 nm), Ga (417.2 nm), Ca (422.7 nm), In (451.1 nm), Tl (535.0 nm), Rb (780.0 nm), and Cs (894.3 nm).

2.2. Reagents

Deionized water (18.2 MΩ cm^{-1}) from a Polwater water purification system (Labopol-Polwater, Poland) was used throughout the study. All chemicals were at least of analytical grade. Stock standard solutions of Ag, Al, Ca, Cd, Cr, Cu, Cs, Fe, Ga, Hg, In, K, Mg, Mn, Na, Pb, Sn, and Zn (1000 mg L^{-1}), obtained from Sigma-Aldrich (Germany), were utilized to prepare all working standard solutions. Solutions of methanol (100%), ethanol (96%), and formic acid (85%), applied for the investigation of the influence of LMWOCs on the signal intensity of the analytes, were provided by Avantor Performance Materials (Poland). To alkalize the FLC solutions, a concentrated TMAH (25% m/m) solution (Sigma-Aldrich, Germany) was employed.

3. Results and discussion

3.1. Emission spectra of the FLC-APGD system for the alkalized FLC solution

At the beginning, the emission spectra of the FLC-APGD system generated in contact with both alkalized and acidified FLC solutions were recorded. The respective blank and standard solutions were analyzed to assess the signal intensity of the background and the selected elements. For the background emission measurements, HNO_3 and TMAH solutions were prepared at their concentrations of 0.01 and 0.1 mol L^{-1}. The emission spectra were recorded in the 200–500 nm range. In the case of the response from the elements, single-element solutions that contained 2 mg L^{-1} of each element were acidified/alkalized with HNO_3/TMAH to a concentration of 0.1 mol L^{-1}. The measurement conditions were as follows: a discharge current of 50 mA and a sample flow rate of 2.5 mL min^{-1}.

Fig. 2 shows the whole recorded range of the emission spectra of FLC-APGD for acidified and alkalized FLC solutions. Fig. S1–S3† show the enlarged aforesaid spectra in the region of the emission of the NO (200–260 nm), OH (280–330 nm), and N_2 (350–450 nm) molecular bands. As can be seen from these figures, generally, the spectra were similar to each other, in terms of both qualitative and quantitative (expressed as the intensity of molecular bands) spectral constituents. However, a few differences between them were noted. First of all, in the 200–240 nm region, the CO bands (the fourth positive $A^1\Pi \rightarrow X^2\Sigma$ system) and the CO^+ bands (the first negative $B^2\Pi \rightarrow {}^2\Sigma$) were observed when the FLC solution was alkalized with TMAH to a concentration of 0.1 mol L^{-1} (see Fig. S1†). The presence of these bands is an obvious result of partial TMAH decomposition in the discharge. It's noteworthy, however, that the same bands were not observed when the solution alkalized with TMAH to 0.01 mol L^{-1} was used. This was likely due to the presence of the NO bands, in the same spectral region, which, therefore, overlapped with the CO and CO^+ bands coming from a more diluted TMAH solution. Secondly, the intensities of the OH bands as well as the H_β line were roughly equal, regardless of the FLC solution composition (see Fig. S2† and 2). This was quite unexpected (especially in the case of the OH bands), considering that TMAH is a strong base. Nevertheless, it could be clarified assuming that the major source of the OH bands in

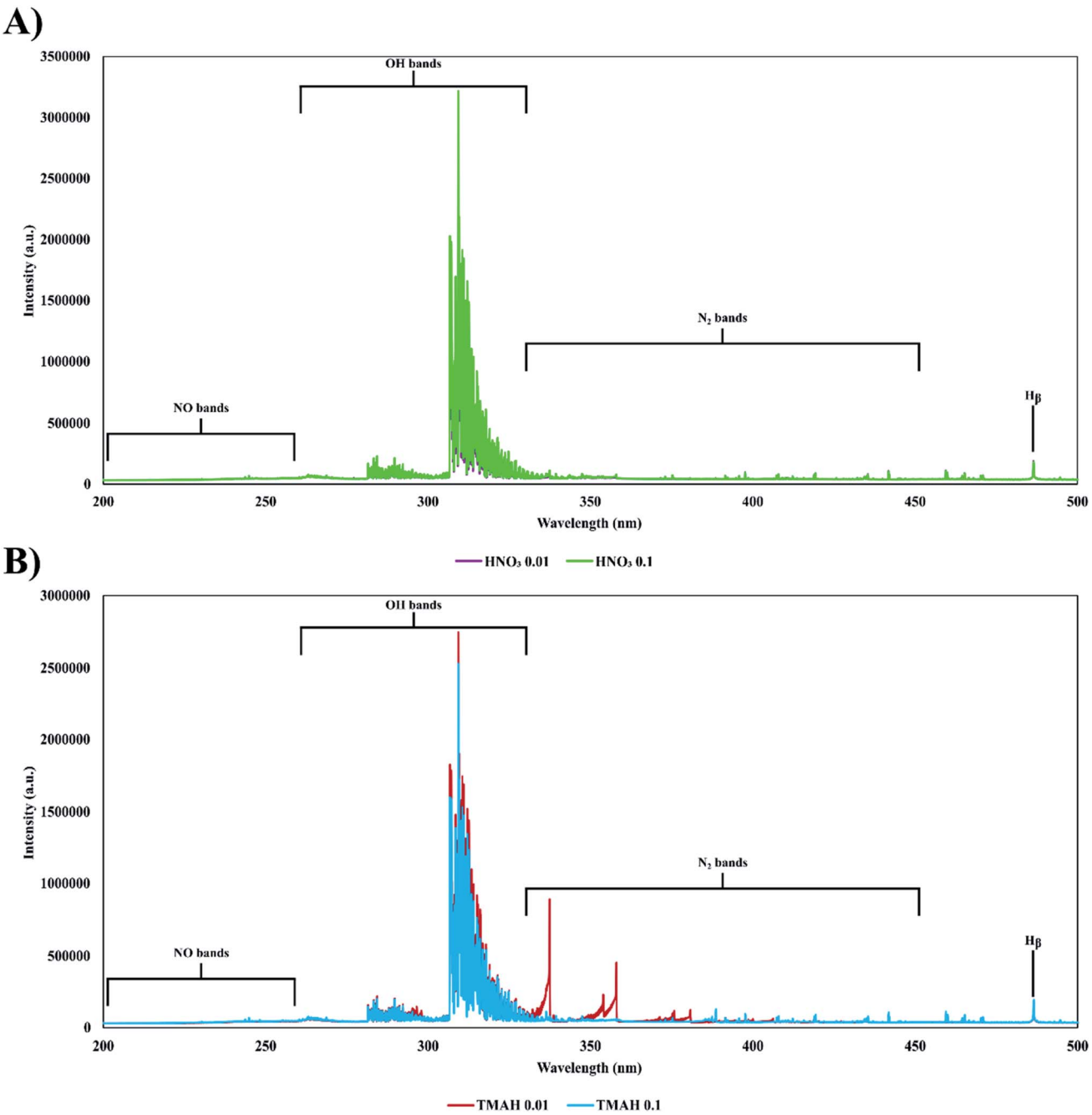

Fig. 2 The emission spectra of the FLC-APGD system generated in contact with HNO_3 (A) and TMAH (B), recorded in the 200–500 nm range.

the FLC-APGD spectrum is water that is evaporated from the FLC solution. As was previously established that the water evaporation varies from 16 to 32% for different FLC-APGD systems,[11,39,40] the participation of the OH species coming from the TMAH dissociation is probably too low to play a significant role in the overall emission from the OH bands. The most noticeable differences in the background emission were, however, found in the 350–400 nm region, where the N_2 molecular band emission is observed (see Fig. S3†). Not only was the intensity of the N_2 molecular bands over 6-fold higher when the FLC solution was alkalized with 0.01 mol L^{-1} TMAH (as compared to other FLC solutions) but also some additional CN bands appeared in the 385–389 nm region when the FLC solution alkalized with 0.1 mol L^{-1} TMAH was used. The explanation of the CN band appearance in the presence of 0.1 mol L^{-1} TMAH is likely related to the TMAH decomposition in the discharge and some probable reactions between C containing species and N_2 molecules. However, the intensification of the N_2 band emission is much more troublesome to clarify, and undoubtedly a more-in-depth study would be necessary to provide a reliable hypothesis. It could be due to an increased diffusion of the air flux into the discharge under these

conditions or some specific excitation conditions for the N_2 molecules that were not observed when a more concentrated TMAH solution was used. Nonetheless, it is worth bearing in mind the intensified N_2 bands when determining Ca, Ga, and Pb in 0.01 mol L^{-1} TMAH as the most prominent lines of these elements are within the spectral region of these molecules.

In the next part of this study, the intensity of the emission lines of different elements was recorded. An attempt was made to choose the elements which would be representatives of various groups and/or general properties. It is noteworthy that K and Na could not be included in this (and any further) study as high signals of these elements (especially in the case of Na) were observed in a blank solution, containing only 0.1 mol L^{-1} TMAH. Therefore, the TMAH solution of higher purity is required for K and Na determination. It was found that the intensity of the emission lines of the studied elements varied ambiguously (see the results displayed in Table 1). Quite small differences between the intensities of the analytical lines of Ag, Fe, Ga, Pb, Rb, and Zn were observed for the acidified and alkalized FLC solutions. However, noticeable variations in the intensity of the analytical lines were noted for the other elements. The intensity of the Ca, Cd Cs, and In lines was higher when the FLC solution was acidified, while a noticeable enhancement of the Hg signal as well as a slight enhancement of the Tl signal were observed for the alkalized solution. The background intensity in the vicinity of the aforementioned analytical lines generally did not significantly differ between acidified and alkalized solutions; therefore, the differences in the signal-to-background ratio (SBR) values for a given element correlate well with the intensity enhancement/drop. Only for Cs and Rb the background intensity was found to drop, by 34 and 42%, respectively, when the FLC solution was alkalized. In the case of Mg, no signal at all was observed for the alkalized solution.

To provide a reliable elucidation of the differences between the analyte signal intensities (or the SBRs), obtained for the acidified and alkalized solutions, the precipitation of hydroxides of certain elements in an alkaline medium must be taken into consideration. Nevertheless, this explanation, obvious howsoever, does not seem to fully clarify all differences. Exemplarily, the precipitate formation of Ag, Fe and Mg was observed during the solution preparation, but only in the case of Mg no signal was observed in the TMAH medium. Moreover, the Fe signal was slightly higher (around 30%) in the alkalized solution, as compared to that in the acidified one. Additionally, the signals of other elements, *e.g.*, Ca and In, also declined, while no precipitates of these elements were visually observed in the solutions neither during their preparation nor after their storage. Also, the signal of Cs was lowered to some extent in the alkaline medium, notwithstanding Cs does not form hydroxide precipitates. It is also worth noting that the TMAH reagent had a strong fishy smell, which means that trimethylamine was present in it, as an impurity. In that case, the formation of some complexes of the studied metals could also possibly take place. Another interesting fact is that the precipitate of Mg was black, meaning that it was not hydroxide. All of this led us to conclude that the lack of significant differences between the signals of certain elements could result from not forming any complexes or precipitates (*e.g.*, Ga and Rb) or possible decomposition of the aforesaid compounds in the discharge (*e.g.*, Ag, Fe, and Pb). On the other hand, the signal enhancement of Hg and Tl could be a result of some volatile species formation in the solutions alkalized with the TMAH reagent. Nevertheless, all the above-mentioned assumptions and hypotheses need a more in-depth study, likely involving the use of some other techniques, *e.g.*, XRD and/or NMR, for determining impurities of the TMAH reagent as well as the kind of precipitate formed during the solution preparation step. Certainly, this goes beyond the main goal of the present work, which was to show the possibility of the FLC-APGD system to stably work with alkaline solutions and determine the element concentrations in such solutions.

However, it could be stated that the results obtained at this stage of research confirm the earlier presumptions[28,29] that the most important factor determining the signal and background intensities is the ionic strength of a solution rather than its pH.

Table 1 The intensity and the signal-to-background ratios (SBRs) for the analytical lines of the studied elements obtained using acidified and alkalized FLC solutions

Element (wavelength)	HNO_3		TMAH	
	Intensity	SBR	Intensity	SBR
Ag (338.3 nm)	9.70×10^5	49.58	8.32×10^5	39.36
Ca (422.7 nm)	5.02×10^4	5.02	1.15×10^4	1.17
Cd (228.8 nm)	1.17×10^5	17.13	4.28×10^4	5.83
Cs (894.3 nm)	2.89×10^5	46.70	1.64×10^5	39.80
Fe (248.3 nm)	1.21×10^4	0.66	1.60×10^4	1.02
Ga (417.2 nm)	1.21×10^5	11.20	1.07×10^5	9.00
Hg (253.7 nm)	9.62×10^3	0.64	3.90×10^4	2.46
In (451.1 nm)	7.42×10^5	53.83	2.81×10^5	24.26
Mg (285.2 nm)	2.14×10^6	64.49	—[a]	—[a]
Pb (368.3 nm)	1.77×10^4	1.39	1.44×10^4	1.17
Rb (780.0 nm)	1.65×10^6	92.83	1.26×10^6	78.63
Tl (535.0 nm)	3.94×10^5	45.13	6.14×10^5	62.33
Zn (213.9 nm)	3.01×10^4	12.42	2.04×10^4	8.28

[a] No signal recorded.

3.2. Optimization of working parameters

In order to reliably compare the analytical characteristics of FLC-APGD generated in contact with alkalized solutions, the optimization of the most influential operating parameters was conducted. The following parameters were identified to have a considerable impact on the analyte signals: the discharge current (20–60 mA), the solution flow rate (1.0–4.0 mL min^{-1}), and the TMAH concentration (0.01–0.1 mol L^{-1}). The number of analytes was reduced in this, and any further, part of this study due to either the unsatisfactory signal intensity of certain elements (Fe, Hg, and Mg) or properties being very similar to other analytes (Cs). Nevertheless, an attempt was made to investigate more diverse groups of elements to provide a general overview of the potential of the developed FLC-APGD-OES method. That being said, the optimization step was carried out using a multi-element standard solution containing Ag, Ca, Cd,

Ga, In, Pb, Rb, Tl, and Zn, all of them at a concentration of 2 mg L^{-1}.

It was shown in our previous studies regarding FLC-APGD generated in contact with acidified solutions[21,26] that the dependence of the abovementioned parameters on each other should be expected. As an example, the discharge current, which could be applied, was restricted by sample acidification as well as the solution flow rate. The discharge instability was noted when both these parameters were not high enough which resulted in the electrical conductivity of the solution being insufficient to support the discharge. As there was no reason to expect otherwise for the alkalized solutions, the multi-parameter optimization was carried out by the design of experiment (DoE) approach. The Box–Behnken response surface design, which comprised 15 runs and included 3 center points, was used for this purpose.[41] The measured response of the system was the SBRs of the analytical lines. A quadratic model was chosen for describing the influence of the investigated operating parameters on the SBR values, nonetheless, insignificant terms (at the significance level $\alpha > 0.15$, meaning the confidence level <85%) were removed from it. In this case, the Box–Behnken design was used to model the curvature in the experimental data with fewer design points. The response surface regression equations (see Table 2) enabled to model how changes in the parameters, *i.e.*, A – the discharge current (mA), B – the solution flow rate (mL min^{-1}), and C – the TMAH concentration (mol L^{-1}), affected the response of interest of the system, the SBR of the analytical lines. These equations were also helpful in finding the levels of the parameters that optimized the response and selecting the operating conditions to meet the specifications. To determine how well the established regression equations fitted the data, the goodness-of-fit statistics is given in Table 3, including values of the coefficient of determination (R^2) that shows the percentage of variation in the response that is explained by the model, values of the adjusted R^2 ($R_{(adj)}{}^2$) that accounts for the terms that are not significant in the model, and values of the predicted R^2 ($R_{(pred)}{}^2$) that determines how well the model predicts responses for new observations. Analyzing the data given in Table 2, it can be stated that the SBR values of the analytical lines of the studied elements generally increased with the increasing discharge current and the TMAH concentration and the decreasing solution flow rate. In the case of the effect of the discharge current and the TMAH concentration, the obtained results are in good agreement with the literature data, obtained for FLC-APGD generated in contact with acidified solutions.[8,21,26,42–44] Regarding the solution flow rate, the outcomes obtained by other researchers are quite ambiguous; some of them observed that the signal intensity (or SBR) increased with the increasing solution flow rate,[17,20,45,46] while others report a signal drop with the increasing solution flow rate.[19,21,47] An initial increase of the signal intensity followed by its subsequent drop was reported as well.[22,48] Nonetheless, the decreasing tendency found herein is in good agreement with the results obtained in our previous paper,[21] in which an almost identical system was studied (the only difference lies in the tungsten rod and tube diameters) but the discharge was generated in contact with the acidified FLC solution. The same observed tendencies of the signal intensity changes with the increasing discharge current and – especially – the TMAH concentration supported the earlier conclusion about the solution ionic strength being the predominant factor

Table 3 The comparison of SBR values predicted by the models and the measured ones[a]

	Goodness-of-fit of models			Model validation		
Analyte	R^2	$R_{(adj)}{}^2$	$R_{(pred)}{}^2$	Predicted	Measured	Relative error (%)
Zn	94.3	91.2	80.1	15.4	12.1	−21.4
Cd	84.8	76.4	47.6	9.2	9.9	+7.6
Ag	99.0	98.0	93.4	53.1	47.6	−10.4
Pb	93.1	89.2	71.6	1.9	1.5	−20.1
Ga	90.2	80.4	51.7	17.6	14.8	−15.9
Ca	96.0	93.0	79.8	1.4	1.3	−7.1
In	63.2	53.2	28.0	24.8	24.6	−0.8
Tl	99.6	99.3	98.4	63.5	65.2	+2.7
Rb	90.7	83.7	66.7	113.5	107.2	−5.6

[a] R^2 – coefficient of determination; $R_{(adj)}{}^2$ – adjusted R^2; $R_{(pred)}{}^2$ – predicted R^2.

Table 2 Statistically significant terms in the regression equations modeling the effect of the studied parameters A, B and C on the signal to background ratio of the analytical lines of Zn, Cd, Ag, Pb, Ga, Ca, In, Tl, and Rb[a]

	Coefficients of regression equation									
Analyte	Const.	A	B	C	A^2	B^2	C^2	$A{\cdot}B$	$A{\cdot}C$	$B{\cdot}C$
Zn	5.23	-1.56×10^{-1}	−1.16	-1.19×10^{1}	4.24×10^{-3}	—	—	—	2.03	—
Cd	−7.70	2.80×10^{-1}	1.83	1.44×10^{2}	—	—	-1.00×10^{3}	-6.88×10^{-2}	—	—
Ag	-1.23×10^{1}	-2.21×10^{-1}	7.98	7.56×10^{2}	1.11×10^{-2}	—	-5.29×10^{3}	-2.21×10^{-1}	6.11	—
Pb	-8.34×10^{-1}	2.55×10^{-2}	2.60×10^{-1}	6.70×10^{-1}	—	—	—	-8.83×10^{-3}	3.33×10^{-1}	—
Ga	-1.96×10^{1}	5.06×10^{-1}	1.29	3.85×10^{2}	—	8.79×10^{-1}	-1.54×10^{3}	-1.25×10^{-1}	—	-3.86×10^{1}
Ca	-9.50×10^{-2}	-1.43×10^{-3}	7.19×10^{-2}	−4.67	—	—	1.34×10^{2}	—	1.81×10^{-1}	−2.44
In	−1.55	5.10×10^{-2}	-5.30×10^{-1}	2.46×10^{2}	—	—	—	—	—	—
Tl	-1.05×10^{1}	1.84×10^{1}	3.64	1.99×10^{2}	—	—	1.05×10^{3}	-9.59×10^{-2}	7.21	—
Rb	-7.27×10^{1}	5.58	-3.0×10^{1}	3.35×10^{3}	-9.60×10^{-2}	—	-2.02×10^{4}	7.92×10^{-1}	—	—

[a] A – discharge current (mA), B – solution flow rate (mL min^{-1}), and C – TMAH concentration (mol L^{-1}).

in determining the analytes signal intensities in the discharge as well as the overall analytical performance of the FLC-APGD system.

As can be seen from Table 3, the goodness-of-fit of the obtained models was reasonably good for most of the elements. Only for In, the R^2 values were significantly impaired. Also, an instability of the In signal was noted for most runs (RSD > 5%), during the optimization step. This might suggest that In occurs in different forms in alkaline solutions, which depends on the base concentration and/or the discharge current. Nevertheless, the comparison of the SBRs of the analytical lines predicted by the model and the measured ones gave, in general, satisfactory results, confirming that the obtained model predicted new data with fair credibility.

For the majority of the studied elements, the optimal conditions predicted by the model were as follows: a discharge current of 60 mA, a solution flow rate of 1.0 mL min^{-1}, and a TMAH concentration of 0.1 mol L^{-1}. However, for Cd, the TMAH concentration providing the highest SBR value was 0.07 mol L^{-1}, whereas the optimal conditions for the determination of Rb were established at a discharge current of 49 mA and a TMAH concentration of 0.09 mol L^{-1}. Nonetheless, the differences in the predicted SBRs values for these elements were relatively low (6.5% for Cd and 26.9% for Rb). Moreover, the stability of the discharge at a discharge current of 60 mA and a solution flow rate of 1.0 mL min^{-1} was quite poor. Therefore, it was decided to apply compromise conditions in the further part of this study, which would still assure high SBR values but with better stability. That being so, a discharge current of 50 mA, a solution flow rate of 1.5 mL min^{-1}, and a TMAH concentration of 0.1 mol L^{-1} were chosen for further experiments for all studied elements.

3.3. Analytical performance

The analytical performance of the studied FLC-APGD generated in contact with the alkalized FLC solutions for the determination of Zn, Cd, Ag, Pb, Ga, Ca, In, Tl, and Rb with the OES detection was evaluated under the compromise conditions given above. For this purpose, the DLs of all analytes, the extent of the linearity of the calibration curves, the sensitivity of the analytical lines, and the precision were assessed. DLs were calculated using $3\sigma/a$, where "3σ" stands for 3 times the standard deviation of 30 consecutive measurements of an appropriate blank solution, and "a" stands for the sensitivity of a corresponding calibration curve. The extent of linearity was investigated using 9 multi-element standard solutions of concentrations changing in the 0.03–10 mg L^{-1} range. The precision was expressed as the relative standard deviation (RSD) for 10 consecutive measurements of a multi-element solution containing 0.1 mg L^{-1} of each analyte. The RSD was measured 3 times and the average results were given.

Table 4 shows the analytical figures of merit achieved by the proposed method. The linearity curves were linear ($R^2 \geq 0.995$) in the whole studied range. Only for Ca, its DL was higher than that for the first studied concentration. Under the compromise conditions, assuring good discharge stability, the RSD of measurements was below 5% for all analytes, with the average close to 2%, indicating very good precision of the developed method. Comparing the DLs of Ga and In obtained herein with those published in our previous work, in which a very similar system was used but the FLC solution was acidified,[26] it can be found that they are higher only 1.7- and 2.7-fold when the FLC solution is alkalized. Bearing in mind the signal intensity differences given in Table 1, it can be stated that in the case of In, the observed DL drop for FLC-APGD generated in contact with the alkalized solutions resulted only from the signal intensity decline. The background level fluctuations in the vicinity of the In analytical line remained the same for both systems, and hence they do not depend on the solution pH. In the case of Ga, the DL is lower than it would result from the signal intensity differences, given in Table 1. This was likely due to the enhanced background level in the vicinity of the Ga analytical line, found for the alkalized FLC solution (see Fig. S3†). That being so, it could be assumed that the variations in the obtained DLs of the remaining elements would be either proportional to the signal intensity ratio listed in Table 1 or slightly worse, in the case of Ca and Pb. In the latter case, the analytical lines of Ca and Pb are observed in the region of enhanced N_2 emission. In fact, the DL of Ca obtained for the acidified FLC solution was determined in our recent study[49] and was equal to 5.7 μg L^{-1}. This means that the DL of Ca obtained

Table 4 The analytical performance of FLC-APGD combined with the OES detection for the determination of Zn, Cd, Ag, Pb, Ga, Ca, In, Tl, and Rb in the solutions alkalized with TMAH

Element	Detection limit (μg L^{-1})	Linearity range (mg L^{-1})	R^2	Sensitivity (a.u. per mg L^{-1})	RSD[a] (%)
Zn	9.7	0.03–10	0.9954	8.92×10^3	3.4
Cd	10	0.03–10	0.9991	1.40×10^4	3.4
Ag	0.81	0.03–10	0.9975	3.22×10^5	1.4
Pb	28	0.03–10	0.9997	4.91×10^3	1.5
Ga	3.0	0.03–10	0.9998	3.82×10^4	4.3
Ca	33	0.05–10	0.9966	3.85×10^3	2.0
In	1.0	0.03–10	0.9996	1.38×10^5	2.8
Tl	0.83	0.03–10	0.9950	2.88×10^5	0.4
Rb	0.35	0.03–10	0.9989	8.88×10^5	1.0

[a] For the analyte concentration of 100 μg L^{-1}.

Table 5 A comparison of the detection limits of Zn, Cd, Ag, Pb, Ga, Ca, In, Tl, and Rb obtained for the proposed FLC-APGD excitation source and other FLC-APGD systems combined with the OES detection (for the past five years)

Detection limit (μg L^{-1})									
Zn	Cd	Ag	Pb	Ga	Ca	In	Tl	Rb	Ref.
9.7	10	0.81	28	3.0	33	1.0	0.83	0.35	This work
10	7.0	2.0	23	—	—	—	—	—	14
50	—	—	—	—	190	—	—	—	16
—	—	—	—	—	96	—	—	2.07	5
72	—	1.2	35	—	—	—	—	0.38	44
140	36	1.4	170	—	—	1.9	—	0.15	4
—	—	—	—	—	—	—	11.8	—	25
—	—	—	—	1.8	—	0.37	—	—	26
—	—	—	—	100	—	16	—	—	46

for the alkalized solution is indeed more impaired than it would be expected, likely due to the enhanced background intensity. On the other hand, when compared to the DLs of elements reported within the last 5 years for other FLC-APGD systems (see Table 5), the DLs obtained in this work are still comparable or (in most cases) better.

Therefore, it can be concluded that quite good DLs, along with relatively wide ranges of the calibration curves linearity and very good precision, make the proposed FLC-APGD system with the alkalized solutions a competitive excitation source for the OES measurements to both other FLC-APGD systems generated in contact with the acidified solutions as well as the commercially available bulky ICP instruments involving high purchasing and operating costs.

3.4. The effect of the addition of low molecular weight organic compounds

LMWOCs such as methanol, ethanol, formic acid, and acetic acid are well known to intensify the response of certain elements and lower their DLs for FLC-APGD generated in contact with the acidified solutions.[15,20,21,45,50] Hence, an attempt was made to evaluate the effect of the abovementioned LMWOCs on the signal intensities of the studied analytes using the alkalized solutions. The impact of methanol, ethanol, formic acid, and acetic acid, at different concentrations varying in the 0.1–10% range, on the signal intensities was investigated using multi-element solutions containing all studied elements at a concentration of 2 mg L^{-1} and one of the studied organic compounds. The intensity of the analytical lines of elements was measured and normalized with regard to a multi-element solution not containing any organic additives. The results are shown in Fig. 3.

Similarly, in the presence of organic compounds in acidified FLC solutions,[21,26] the discharge became unstable at higher concentrations of methanol (>5%) and ethanol (>3%) but it could be maintained over the whole studied range of concentrations of the organic acids. However, lower visual stability as well as impaired precision for certain elements were noted at an acid concentration of 10% and the highest possible-to-study concentrations of methanol and ethanol. The impact of methanol on the signal intensities of the studied analytes was similar for the majority of them – a constant signal drop was observed with the increasing concentration of this compound. The most vulnerable to the presence of methanol in the analyzed solution were Cd, Ag, and In, whose signals were lowered up to 35–42%. The only exception to this rule was Tl, whose signals were meaningfully boosted (up to 4-fold) with increasing concentration of methanol. In the presence of ethanol only Cd, In, and Tl behaved similarly (as compared to the outcomes obtained for methanol); in the latter case, the signal enhancement was even greater (up to 6-fold), even though the highest studied concentration was lower (compared to the highest studied concentration of methanol). The signal intensities of the remaining elements were roughly constant either over the whole concentration range (Zn, Ag, Ga, and Rb) or up to the ethanol concentration of 1% (Pb and Ca). Nevertheless, the signal intensity of Zn was slightly enhanced in the presence of ethanol, while the signal intensity of Rb was rather declined.

Entirely distinct outcomes were observed when organic acids were added into the FLC solution. For the vast majority of the studied elements, the signal intensity drop was noted up to acid concentrations of 0.3, 0.5 or 1%, followed by its subsequent increase. The most spectacular signal intensity enhancements were observed for Zn, Cd, Ag, Pb, and In (up to 5-, 6-, 6-. 8-, and 6-fold, respectively). For these analytes, the highest signal intensity was obtained usually for an acid concentration of 10% and usually this effect was stronger for formic acid. Slight signal intensity enhancements were also noted for Ga, Ca, and Tl (up to 1.6-fold) but only in the presence of higher concentrations of formic acid. These observations are in good agreement with the results reported by Doroski *et al.*,[51] indicating that the signal enhancement is found particularly for the volatile species forming elements, *e.g.*, Ag, Hg, or Pb. As these elements are known to form different kinds of volatile species, it was hypothesized that the formation of some kind of such species is the process that happens when formic or acetic acids are added into the FLC solution containing such elements.

Considering that the CO and CO^+ bands were identified in the spectra of FLC-APGD generated in contact with solutions alkalized with TMAH, while a slight increase of the OH and N_2 emission bands was observed for higher concentrations of the previously studied organic additives,[21,52] this slight enhancement of the remaining analyte signals could be attributed to an impact of organic acids on the excitation conditions in the discharge. All of this would again support the assumption of the pH-independence of FLC-APGD, in reference to its analytical response. Nevertheless, the impact of pH is actually worth considering here. First of all, when adding any acid to alkaline solutions, it is to be expected that the base will be neutralized and that is what likely happened herein for lower organic acid concentrations. Therefore, the initial signal drop is probably due to the decline of the TMAH concentration, being the result of its neutralization in the presence of a given organic acid. Apparently, when the concentration of organic acids is equal or above 1%, TMAH was likely fully neutralized and the actual

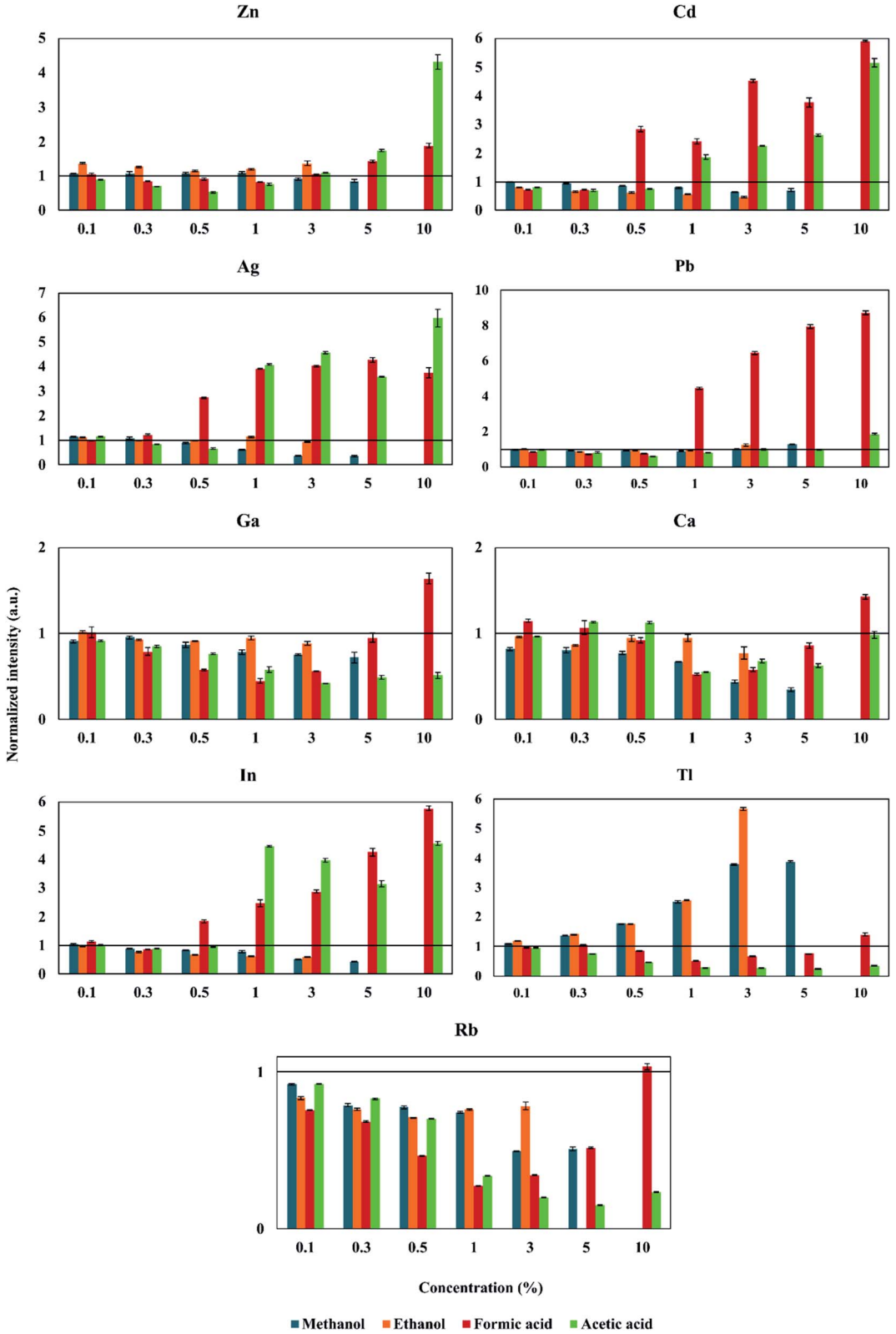

Fig. 3 The effect of the studied organic compounds on the intensity (normalized with regard to the signal intensity obtained for the solution without any organic additives) of the analytical lines of Zn, Cd, Ag, Pb, Ga, Ca, In, Tl, and Rb. The missing bars are due to the plasma instability under given conditions, which precluded taking the measurements.

solution composition was then a solution consisting excess of formic/acetic acid and the product of the TMAH neutralization. Therefore, it could be assumed that the observed signal intensity enhancement was related to the presence of organic acids themselves; hence, it was pH-independent as long as the excess of a given acid was assured.

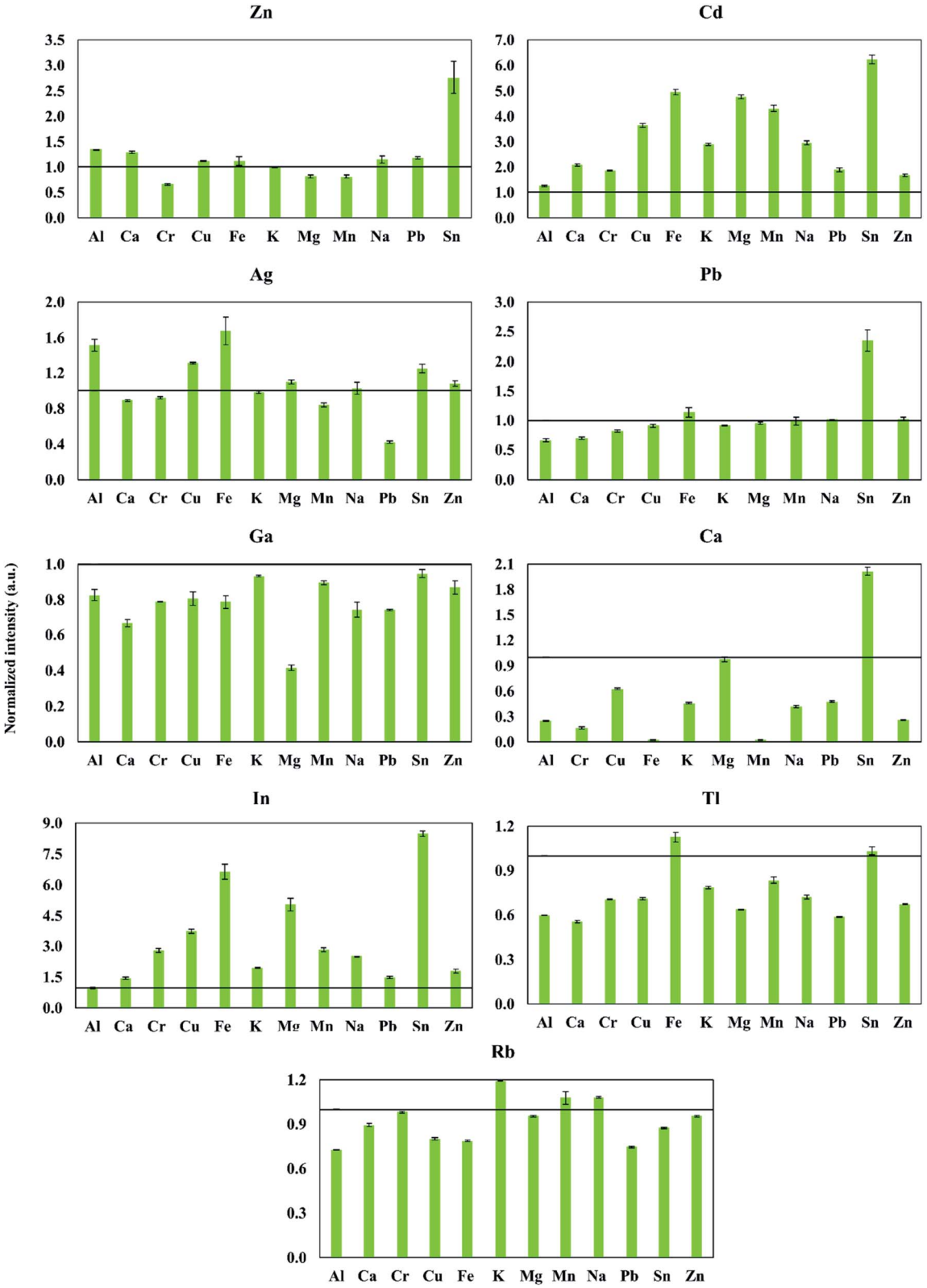

Fig. 4 The effect of foreign elements (at a concentration of 50 mg L^{-1}) on the recovery (determined by comparing the signals relative to those obtained for the solution without any interfering ions) of Zn, Cd, Ag, Pb, Ga, Ca, In, Tl, and Rb (at a concentration of 2 mg L^{-1}).

Another parameter which is worth considering with reference to the pH-dependence is the enhancement factors of Zn and In as they are clearly more noticeable than those of other elements that also do not form volatile species. Yu *et al.*[22] and our group[26] investigated the impact of the same organic acids on the signal intensities of Zn and In, respectively, for FLC-APGD generated in contact with acidified solutions. In both these studies, no signal enhancement or drop was observed, clearly indicating that in the acidic medium there is no impact of these acids on the response of Zn and In. Considering the fact that after the addition of the excess of formic/acetic acid to the alkalized solution its pH is still acidic, it is likely that the difference between the response of Zn and In, obtained in the current work and the previous ones, lies in Zn and In species that are being formed in (generally) alkalized or (specifically) TMAH solutions. Apparently, in alkalized FLC solutions, Zn and In possibly form other types of compounds (compared to simple cations supposedly formed in the acidified solutions) that are more efficiently transported to the discharge when organic acids are present in the analyzed sample. Although the dissolution of some possible precipitates of both analytes in added organic acids could also be responsible for their signal enhancement, this hypothesis is less likely in our opinion as, firstly, no such Zn and In precipitates were observed during this research and secondly, a similar signal enhancement effect would then be expected for other elements (exemplarily Ca).

To sum up all the above described observations, it seems that, generally, the effect of the addition of organic compounds on the analyte signals intensity does not really differ for the alkalized solutions, from that observed for the acidified solutions, except for Zn and In in the presence of formic and acetic acids added to the FLC solution. Therefore, in the majority of cases, this effect is pH-independent and when some dependency occurs, it is rather due to the specific properties of a particular element rather than, for instance, the impact of the alkalized solution on the excitation conditions in the discharge.

3.5. The effect of foreign ions

Since it is believed that the analyte transportation to the discharge in the FLC-APGD system takes place by bombarding the surface of the FLC solution with positive ions, it is to be expected that all solution constituents are carried into the discharge phase and may influence the analyte signals, *e.g.*, by changing the excitation conditions in the plasma. With regard to this, the insusceptibility of the developed FLC-APGD-OES method to the interferences coming from concomitant elements, commonly occurring in real samples, was studied. The impact of the presence of Al, Ca, Cr, Cu, Fe, K, Mg, Mn, Na, Sn, and Zn, at a concentration of 50 mg L^{-1}, on the signal intensities of the analytical lines was determined. To achieve this, each of the aforesaid concomitant ions was added separately to a multi-element solution containing Zn, Cd, Ag, Pb, Ga, Ca, In, Tl, and Rb, each at a concentration of 2 mg L^{-1}. Interestingly enough, as the concentration of the concomitant ions was relatively high, the color changes/precipitate formation, after TMAH addition to solutions containing appropriate amounts of the stock standard solutions of the concomitant ions, were easily observed (in contrast to the earlier stages of this research, when significantly lower amounts of standard solutions were used). Thus, after the addition of TMAH to the concomitant ion solutions, the formation of black precipitates was noted for Mg and Mn, whereas the solutions of Ca, Cu, and Fe became yellow, blue and orange, respectively. No precipitate formation was observed shortly after the sample preparation; nevertheless, they were observed for Cu and Fe the next day.

The measured signal intensities of the analytical lines were normalized in regard to the signal intensities obtained for a multi-element solution of the analytes, which did not contain any of the foreign ions and served as a reference solution. The obtained outcomes are depicted in Fig. 4. As can be seen from the figure, noticeable matrix effects were observed for almost all analytes. The signals of Zn, Pb, Ga, and Rb remained relatively unaffected by the presence of the majority of the studied foreign ions; however, none from the analytes was insusceptible to all of them. Exemplarily, the signal intensity of the Zn analytical line was almost 3-fold higher in the presence of Sn and about 30% lower in the presence of Cr. The signal of Pb was significantly enhanced in the presence of Sn, whereas the signal intensity of the Ga analytical line was suppressed in the presence of Mg. On the other hand, the signals of Cd and In were increased in the presence of each of the concomitant ions, particularly, when Sn was added to the solution, which resulted in a 6.2- (Cd) and 8.5-fold (In) signal intensity boost. Substantial signal intensity enhancement caused by the inference of Sn was also observed for Zn, Pb, and Ca.

Comparing the results for Ga and In obtained herein with those from our previous work,[26] huge differences in the analyte behavior are noted, especially in the case of In. For the acidified FLC solution, only small matrix effects were observed for In, while for Ga these effects were a little greater, but its response was rather enhanced than reduced.

Providing a reliable justification regarding the reasons of such intense matrix effects observed in FLC-APGD generated from the alkalized solutions would be troublesome and was beyond the scope of this work. Nevertheless, they are certainly related to the reactions taking place in the alkalized solutions and/or with TMAH (or its impurities), *e.g.*, the formation of precipitates of the interferents and the adsorption of the analyte ions by these precipitates. Regardless of a specific reason for the observed outcomes, there is no doubt that the application of the proposed method for a real sample analysis requires the standard addition method for calibration.

4. Conclusions

In this work, the performance of FLC-APGD generated in contact with the alkalized solution for the determination of Zn, Cd, Ag, Pb, Ga, Ca, In, Tl, and Rb was investigated and the obtained results were compared to those obtained for the discharge system operated in contact with the acidified solutions. It was found that the analyte signals are present in the FLC-APGD spectrum, regardless of the pH of the FLC solution. The analyte response was usually higher when the FLC solution

was acidified; however, the signals of Fe, Hg, and Tl were still greater for the alkalized solutions. The solution alkalization did not significantly change the background level as well; however, additional spectral constituents, namely the CO, CO^+, and CN bands, were observed for a higher TMAH concentration. It was also established that the proposed method is not suitable for the Mg determination at concentrations equal or lower than 2 mg L^{-1} (higher concentrations were not studied), while the determination of K and Na requires a reagent of higher purity.

The abovementioned lack of substantial differences in the FLC-APGD spectra, along with all similarities noted during the optimization step as well as the effects observed after the addition of both inorganic and organic constituents into the alkalized FLC solutions, led us to a conclusion that, generally, the performance of the FLC-APGD system (with the OES detection) depended on the ionic strength of the FLC solution rather than its pH. Nevertheless, possible reactions of the analytes with the conductive electrolyte need to be taken into account as they seemed to be the only factor responsible for differentiated outcomes noted between the acidified and alkalized FLC solutions.

We believe that the results obtained herein pointed out a few interesting issues regarding the operation of FLC-APGD in contact the alkalized solutions. Although a reliable clarification of some of them could not be provided in this work, the observations and conclusions presented in this work could contribute to the further development of the FLC-APGD systems. That being said, this study could be a starting point for improving the analytical performance of the FLC-APGD system by providing the electrical conductivity with other electrolytes, *e.g.*, bases, salts, *etc.* Although some part of such a kind of study had been done previously, certainly there is lack of comprehensive approach to that matter.

Even though the analytical figures of merit (particularly the DLs) determined in this work supposedly (certainly for Ga and In) were slightly lower than those obtained in the case of the acidified solutions, they were still better than the majority of the DLs reported by other researchers dealing with FLC-APGD in the last five years. Hence, the developed FLC-APGD system seems to be a competitive excitation source to commercially available large-scale instrumentation such as ICP. Notwithstanding, the proposed method required the application of the standard addition method for calibration, the digestion procedure with the aid of TMAH had been previously established to be much faster and equally effective than in the case of the application of HNO_3 and other mineral acids. In addition, as opposed to the ICP-OES method, there is no issue with the delivering of solutions containing precipitates into the discharge; therefore the sample solutions do not need to be centrifuged if the precipitate formation is observed during the sample preparation step. Moreover, the developed FLC-APGD system provides the advantages of small size, no gas consumption, and low manufacturing and operating costs.

Conflicts of interest

There are no conflicts to declare.

References

1 Z. Wang, R. Gai, L. Zhou and Z. Zhang, Design modification of a solution-cathode glow discharge-atomic emission spectrometer for the determination of trace metals in titanium dioxide, *J. Anal. At. Spectrom.*, 2014, **29**, 2042–2049.
2 P. Pohl, P. Jamroz, K. Swiderski, A. Dzimitrowicz and A. Lesniewicz, Critical evaluation of recent achievements in low power glow discharge generated at atmospheric pressure between a flowing liquid cathode and a metallic anode for element analysis by optical emission spectrometry, *Trends Anal. Chem.*, 2017, **88**, 119–133.
3 K. Swiderski, P. Pohl and P. Jamroz, A miniaturized atmospheric pressure glow microdischarge system generated in contact with a hanging drop electrode – a new approach to spectrochemical analysis of liquid microsamples, *J. Anal. At. Spectrom.*, 2019, **34**, 1287–1293.
4 A. J. Schwartz, S. J. Ray, G. C.-Y. Chan and G. M. Hieftje, Spatially resolved measurements to improve analytical performance of solution-cathode glow discharge optical-emission spectrometry, *Spectrochim. Acta, Part B*, 2016, **125**, 168–176.
5 P. Zheng, W. Li, J. Wang, X. Zhai, X. Mao, X. Wang and C. Lai, Spatially Resolved Characteristics of Solution Cathode Glow Discharge Source Coupled with an Interference Filter Wheel as Spectral Discrimination Device, *Anal. Lett.*, 2020, **53**, 31–39.
6 T. Cserfalvi, P. Mezei and P. Apai, Emission studies on a glow discharge in atmospheric pressure air using water as a cathode, *J. Phys. D: Appl. Phys.*, 1993, **26**, 2184–2188.
7 B. K. Zuev, V. V. Yagov, M. L. Getsina and B. A. Rudenko, Discharge on Boiling in a Channel as a New Atomization and Excitation Source for the Flow Determination of Metals by Atomic Emission Spectrometry, *J. Anal. At. Spectrom.*, 2002, **57**, 907–911.
8 M. R. Webb, F. J. Andrade, G. Gamez, R. McCrindle and G. M. Hieftje, Spectroscopic and electrical studies of a solution-cathode glow discharge, *J. Anal. At. Spectrom.*, 2005, **20**, 1218–1225.
9 P. Jamroz and W. Zyrnicki, Spectroscopic Characterization of Miniaturized Atmospheric-Pressure dc Glow Discharge Generated in Contact with Flowing Small Size Liquid Cathode, *Plasma Chem. Plasma Process.*, 2011, **31**, 681–696.
10 X. Liu, Z. Zhu, D. He, H. Zheng, Y. Gan, N. Stanley Belshaw, S. Hu and Y. Wang, Highly sensitive elemental analysis of Cd and Zn by solution anode glow discharge atomic emission spectrometry, *J. Anal. At. Spectrom.*, 2016, **31**, 1089–1096.
11 K. Greda, K. Swiderski, P. Jamroz and P. Pohl, Flowing Liquid Anode Atmospheric Pressure Glow Discharge as an Excitation Source for Optical Emission Spectrometry with the Improved Detectability of Ag, Cd, Hg, Pb, Tl, and Zn, *Anal. Chem.*, 2016, **88**, 8812–8820.
12 P. Jamroz, K. Greda, A. Dzimitrowicz, K. Swiderski and P. Pohl, Sensitive Determination of Cd in Small-Volume Samples by Miniaturized Liquid Drop Anode Atmospheric

Pressure Glow Discharge Optical Emission Spectrometry, *Anal. Chem.*, 2017, **89**, 5729–5733.

13 P. Pohl, P. Jamroz, K. Greda, M. Gorska, A. Dzimitrowicz, M. Welna and A. Szymczycha-Madeja, Five years of innovations in development of glow discharges generated in contact with liquids for spectrochemical elemental analysis by optical emission spectrometry, *Anal. Chim. Acta*, 2021, 338399.

14 X. Peng, X. Guo, F. Ge and Z. Wang, Battery-operated portable high-throughput solution cathode glow discharge optical emission spectrometry for environmental metal detection, *J. Anal. At. Spectrom.*, 2019, **34**, 394–400.

15 J. Yu, L. Yin, Q. Lu, F. Feng, Y. Kang and H. Luo, Highly sensitive determination of mercury by improved liquid cathode glow discharge with the addition of chemical modifiers, *Anal. Chim. Acta*, 2020, **1131**, 25–34.

16 J. Yu, S. Yang, D. Sun, Q. Lu, J. Zheng, X. Zhang and X. Wang, Simultaneously determination of multi metal elements in water samples by liquid cathode glow discharge-atomic emission spectrometry, *Microchem. J.*, 2016, **128**, 325–330.

17 Q. Lu, H. Luo, J. Yu, Y. Kang, Z. Lu, J. Li and W. Yang, Evaluation of a sampling system coupled to liquid cathode glow discharge for the determination of rubidium, cesium and strontium in water samples, *Microchem. J.*, 2020, **158**, 105246.

18 C. Yang, L. Wang, Z. Zhu, L. Jin, H. Zheng, N. Stanley Belshaw and S. Hu, Evaluation of flow injection-solution cathode glow discharge-atomic emission spectrometry for the determination of major elements in brines, *Talanta*, 2016, **155**, 314–320.

19 P. Zheng, Y. Chen, J. Wang and S. Xue, A pulsed atmospheric-pressure discharge generated in contact with flowing electrolyte solutions for metal element analysis by optical emission spectrometry, *J. Anal. At. Spectrom.*, 2016, **31**, 2037–2044.

20 J. Yu, Y. Kang, Q. Lu, H. Luo, Z. Lu, L. Cui and J. Li, Improvement of analytical performance of liquid cathode glow discharge for the determination of bismuth using formic acid as a matrix modifier, *Microchem. J.*, 2020, **159**, 105507.

21 M. Gorska, K. Greda and P. Pohl, Determination of bismuth by optical emission spectrometry with liquid anode/cathode atmospheric pressure glow discharge, *J. Anal. At. Spectrom.*, 2021, **36**, 165–177.

22 J. Yu, X. Zhang, Q. Lu, X. Wang, D. Sun, Y. Wang and W. Yang, Determination of calcium and zinc in gluconates oral solution and blood samples by liquid cathode glow discharge-atomic emission spectrometry, *Talanta*, 2017, **175**, 150–157.

23 J. Yu, X. Zhang, Q. Lu, L. Yin, F. Feng, H. Luo and Y. Kang, Liquid Cathode Glow Discharge as an Excitation Source for the Analysis of Complex Water Samples with Atomic Emission Spectrometry, *ACS Omega*, 2020, **5**, 19541–19547.

24 R. Shekhar, D. Karunasagar, M. Ranjit and J. Arunachalam, Determination of elemental constituents in different matrix materials and flow injection studies by the electrolyte cathode glow discharge technique with a new design, *Anal. Chem.*, 2009, **81**, 8157–8166.

25 W. Zu, Y. Wang, X. Yang and C. Liu, A portable solution cathode glow discharge-atomic emission spectrometer for the rapid determination of thallium in water samples, *Talanta*, 2017, **173**, 88–93.

26 M. Gorska and P. Pohl, Comparison of the performance of atmospheric pressure glow discharges operated between a flowing liquid cathode and either a pin-type anode or a helium jet anode for the Ga and In determination by the optical emission spectrometry, *Talanta*, 2021, **226**, 122155.

27 P. Mezei, T. Cserfalvi, H. J. Kim and M. A. Mottaleb, The influence of chlorine on the intensity of metal atomic lines emitted by an electrolyte cathode atmospheric glow discharge, *Analyst*, 2001, **126**, 712–714.

28 B. K. Zuev, V. V. Yagov and A. S. Grachev, Discharge in liquids as a spectral source of radiation: Effect of the supporting electrolyte on the intensity of metal lines, *J. Anal. Chem.*, 2008, **63**, 586–589.

29 V. V. Yagov and M. L. Gentsina, Effect of Supporting Electrolyte Composition on the Intensity of Metal Lines in Electrolyte-Cathode Discharge Spectra, *J. Anal. Chem.*, 2004, **59**, 64–70.

30 A. S. Ribeiro, A. L. Moretto, M. A. Z. Arruda and S. Cadore, Analysis of Powdered Coffee and Milk by ICP OES after Sample Treatment with Tetramethylammonium Hydroxide, *Microchim. Acta*, 2003, **141**, 149–155.

31 F. S.-S. Chien, W.-F. Hsieh, S. Gwo, A. E. Vladar and J. A. Dagata, Silicon nanostructures fabricated by scanning probe oxidation and tetra-methyl ammonium hydroxide etching, *J. Appl. Phys.*, 2002, **91**, 10044.

32 S. Simon, M. Bueno, G. Lespes, M. Mench and M. Potin-Gautier, Extraction procedure for organotin analysis in plant matrices: optimisation and application, *Talanta*, 2002, **57**, 31–43.

33 K. Kuroda, N. Nishimura, A. Izumi and D. R. Dimmel, Pyrolysis of lignin in the presence of tetramethylammonium hydroxide: a convenient method for S/G ratio determination, *J. Agric. Food Chem.*, 2002, **50**, 1022–1027.

34 L. Grasset, C. Guignard and A. Ambles, Free and esterified aliphatic carboxylic acids in humin and humic acids from a peat sample as revealed by pyrolysis with tetramethylammonium hydroxide or tetraethylammonium acetate, *Org. Geochem.*, 2002, **33**, 181–188.

35 J. Pereira Dos Santos Alves, U. Mozart Ferreira Da Mata Cerqueira, C. Galvao Novaes, J. Alves Barreto, J. Dos Santos Trindade, S. Alves Araujo and M. Almeida Bezerra, An alkaline dissolution-based method using tetramethylammonium hydroxide for metals determination in cow milk samples, *Food Chem.*, 2021, **334**, 127559.

36 B. L. Batista, J. L. Rodrigues, J. A. Nunes, L. Tormen, A. J. Curtius and F. Barbosa, Simultaneous determination of Cd, Cu, Mn, Ni, Pb and Zn in nail samples by inductively coupled plasma mass spectrometry (ICP-MS) after tetramethylammonium hydroxide solubilization at

room temperature: comparison with ETAAS, *Talanta*, 2008, **76**, 575–579.

37 F. Barbosa Jr, C. D. Palmer, F. J. Krug and P. J. Parsons, Determination of total mercury in whole blood by flow injection cold vapor atomic absorption spectrometry with room temperature digestion using tetramethylammonium hydroxide, *J. Anal. At. Spectrom.*, 2004, **19**, 1000–1005.

38 L. Murthy, E. E. Menden, P. M. Eller and H. G. Petering, Atomic absorption determination of zinc, copper, cadmium, and lead in tissues solubilized by aqueous tetramethylammonium hydroxide, *Anal. Biochem.*, 1973, **53**, 365–372.

39 K. Swiderski, A. Dzimitrowicz, P. Jamroz and P. Pohl, Influence of pH and low-molecular weight organic compounds in solution on selected spectroscopic and analytical parameters of flowing liquid anode atmospheric pressure glow discharge (FLA-APGD) for the optical emission spectrometric (OES) determination of Ag, Cd, and Pb, *J. Anal. At. Spectrom.*, 2018, **33**, 437–451.

40 M. Yuan, X. Peng, F. Ge, Q. Li, K. Wang, D.-G. Yu and Z. Wang, Simplified design for solution anode glow discharge atomic emission spectrometry device for highly sensitive detection of Ag, Bi, Cd, Hg, Pb, Tl, and Zn, *Microchem. J.*, 2020, **155**, 104785.

41 K. Greda, K. Kurcbach, K. Ochromowicz, T. Lesniewicz, P. Jamroz and P. Pohl, Determination of mercury in mosses by novel cold vapor generation atmospheric pressure glow microdischarge optical emission spectrometry after multivariate optimization, *J. Anal. At. Spectrom.*, 2015, **30**, 1743–1751.

42 P. Zheng, X. Zhai, J. Wang and P. Tang, Analytical Characterization of a Solution Cathode Glow Discharge with an Interference Filter Wheel for Spectral Discrimination, *Anal. Lett.*, 2018, **51**, 2304–2315.

43 T. Cserfalvi and P. Mezei, Direct solution analysis by glow discharge: electrolyte-cathode discharge spectrometry, *J. Anal. At. Spectrom.*, 1994, **9**, 345–349.

44 J. Wang, P. Tang, P. Zheng and X. Zhai, Analysis of metal elements by solution cathode glow discharge-atomic emission spectrometry with a modified pulsation damper, *J. Anal. At. Spectrom.*, 2017, **32**, 1925–1931.

45 Q. Lu, F. Feng, J. Yu, L. Yin, Y. Kang, H. Luo, D. Sun and W. Yang, Determination of trace cadmium in zinc concentrate by liquid cathode glow discharge with a modified sampling system and addition of chemical modifiers for improved sensitivity, *Microchem. J.*, 2020, **152**, 104308.

46 J. Yu, Y. Kang, Q. Lu, H. Luo, L. Cui, Z. Lu and J. Li, Determination of gallium and indium by solution cathode glow discharge as an excitation source for atomic emission spectrometry, *Spectrochim. Acta, Part B*, 2020, **172**, 105968.

47 P. Zheng, W. Li, J. Wang, N. Wang, C. Zhong, Y. Luo, X. Wang, X. Mao and C. Lai, Analytical Performance of Hollow Anode-Solution Cathode Glow Discharge-Atomic Emission Spectrometry, *Anal. Lett.*, 2020, **53**, 693–704.

48 H. Yuan, D.-Z. Yang, X. Li, L. Zhang, X.-F. Zhou, W.-C. Wang and Y. Xu, A pulsed electrolyte cathode discharge used for metal element analysis by atomic emission spectrometry, *Phys. Plasmas*, 2019, **26**, 53505.

49 M. Gorska and P. Pohl, Simplified and rapid determination of Ca, K, Mg, and Na in fruit juices by flowing liquid cathode atmospheric glow discharge optical emission spectrometry, *J. Anal. At. Spectrom.*, 2021, **36**, 1455–1465.

50 Y.-J. Zhou, J. Ma, F. Li, T. Xian, Q.-H. Yuan and Q.-F. Lu, Sensitivity improvement of solution cathode glow discharge-optical emission spectrometry by external magnetic field for optical determination of elements, *Microchem. J.*, 2020, **158**, 105224.

51 T. A. Doroski and M. R. Webb, Signal enhancement in solution-cathode glow discharge — optical emission spectrometry *via* low molecular weight organic compounds, *Spectrochim. Acta, Part B*, 2013, **88**, 40–45.

52 Q. Xiao, Z. Zhu, H. Zheng, H. He, C. Huang and S. Hu, Significant sensitivity improvement of alternating current driven-liquid discharge by using formic acid medium for optical determination of elements, *Talanta*, 2013, **106**, 144–149.